14-3-3ζ: A suppressor of inflammatory arthritis

Joshua Kim[a], Krista Chun[a], Jenna McGowan[a], Youjie Zhang[a], Piotr J. Czernik[a], Blair Mell[a], Bina Joe[a], Saurabh Chattopadhyay[b], Joseph Holoshitz[c], and Ritu Chakravarti[a,1]

[a]Department of Physiology and Pharmacology, College of Medicine and Life Sciences, University of Toledo, Toledo, OH 43614; [b]Department of Medical Microbiology and Immunology, College of Medicine and Life Sciences, University of Toledo, Toledo, OH 43614; and [c]Department of Internal Medicine, University of Michigan, Ann Arbor, MI 48109

Inflammatory arthritis (IA) is a common disease that affects millions of individuals worldwide. Proinflammatory events during IA pathogenesis are well studied; however, loss of protective immunity remains underexplored. Earlier, we reported that 14-3-3zeta (ζ) has a role in T-cell polarization and interleukin (IL)-17A signal transduction. Here, we demonstrate that 14-3-3ζ knockout (KO) rats develop early-onset severe arthritis in two independent models of IA, pristane-induced arthritis and collagen-induced arthritis. Arthritic 14-3-3ζ KO animals showed an increase in bone loss and immune cell infiltration in synovial joints. Induction of arthritis coincided with the loss of anti-14-3-3ζ antibodies; however, rescue experiments to supplement the 14-3-3ζ antibody by passive immunization did not suppress arthritis. Instead, 14-3-3ζ immunization during the presymptomatic phase resulted in significant suppression of arthritis in both wild-type and 14-3-3ζ KO animals. Mechanistically, 14-3-3ζ KO rats exhibited elevated inflammatory gene signatures at the messenger RNA and protein levels, particularly for IL-1β. Furthermore, the immunization with recombinant 14-3-3ζ protein suppressed IL-1β levels, significantly increased anti-14-3-3ζ antibody levels and collagen production, and preserved bone quality. The 14-3-3ζ protein increased collagen expression in primary rat mesenchymal cells. Together, our findings indicate that 14-3-3ζ causes immune suppression and extracellular remodeling, which lead to a previously unrecognized IA-suppressive function.

14-3-3zeta | inflammatory arthritis | Il-1beta | bone loss | collagen

Rheumatoid arthritis (RA) is a chronic autoimmune disease associated with increased innate and adaptive immune responses (1, 2). Antigens activate T and B cells, leading to increased production of cytokines and antibodies, a characteristic of seropositive RA (3, 4). Increased rheumatoid factor and anticitrullinated antibodies correlate with RA disease activity. However, the loss of protective autoantibodies or autoantigens in immune diseases remains unclear (5–7). It is suggested that autoantibody can deplete antigens or activate complement pathways to produce immune suppression (8, 9). Therefore, the disruption of homeostasis between natural antibodies and target antigen expression generates a bias in favor of pathogenic pathways responsible for autoimmune diseases (7). In the absence of antigen-based protective immunity, autoantigens can promote pathogenesis, either directly or by neutralizing protective mechanisms (10). Most autoantigens in RA are cytosolic proteins exposed to the external environment due to cell death or NETosis (11–13). Antigen-stimulated innate and adaptive immune responses often support inflammation (2, 14). However, antigen-specific immunotherapy has emerged as a promising strategy in treating autoimmune diseases (15, 16). Several clinical trials are testing for induction of antigen-specific tolerance in RA (17, 18). Therefore, it is important to understand the role of protective mechanisms responsible for RA suppression.

The 14-3-3ζ protein is an adaptor that regulates cellular signaling by binding to a wide range of proteins (19–22). Changes in 14-3-3ζ expression levels are associated with cancer and neurological and cardiovascular pathologies (23). The 14-3-3ζ genetic variants exhibit RASOpathies, particularly the cardiofaciocutaneous

syndrome (24). Recent literature shows that 14-3-3ζ regulate immune responses via antigen presentation and extracellular signaling (25–30). We previously reported that 14-3-3ζ is an antigen in thoracic aortic aneurysms associated with large vessel vasculitis and promotes human T-cell polarization in favor of T helper (Th)1 and Th17 cells (31, 32). This led us to hypothesize that 14-3-3ζ's immunogenic function has pathologic autoimmune consequences. To test our hypothesis, we investigated the role of 14-3-3ζ and its antigenic function in animal models of inflammatory arthritis (IA).

We assessed the effect of 14-3-3ζ on IA on 8-wk-old arthritis-susceptible Lewis (LEW) rats (33–35) that were intradermally injected with either pristane or type-II collagen to induce pristane-induced arthritis (PIA) or collagen-induced arthritis (CIA), respectively. Wild-type (WT) and global 14-3-3ζ knockout (KO) LEW rats were used in the study to examine the function of endogenous 14-3-3ζ. Furthermore, animals were immunized with incomplete Freund's adjuvant (IFA) mixed with purified 14-3-3ζ to study its immunogenic role in IA progression. Contrary to the hypothesis, 14-3-3ζ KO rats developed severe joint inflammation and lost a significant amount of bone and body weight when tested in PIA and CIA models. Importantly, we observed that 14-3-3ζ immunization reduced joint inflammation while preserving bone and body weight. A negative trend was found between circulating 14-3-3ζ antibody levels and inflammatory arthritis scores. However, replenishing the antibody by passive immunization was ineffective in suppressing the inflammation, suggesting that suppression of arthritis required an active immunogenic function of 14-3-3ζ. The

Significance

Inflammatory arthritis (IA) affects more than 1% of the world population. Natural host-protective immune responses to suppress or prophylactic immunization to prevent IA remain unknown. We previously showed that 14-3-3ζ is an auto-antigen in large vessel vasculitis. In the current study, we examined the role of antigenic 14-3-3ζ using animal models of IA. Our results showed that 14-3-3ζ is an endogenous suppressor of IA. In addition to immunological manipulations, 14-3-3ζ has a strong effect on bone remodeling. Moreover, we developed a 14-3-3ζ–based prophylactic vaccine that reduces IA symptoms. This report shows the host-protective role of antigenic 14-3-3ζ in IA suppression and shows that autoantigens play an important role in inflammatory diseases.

www.manaraa.com

long-term effects of 14-3-3ζ immunization included suppressing proinflammatory cytokines and promoting collagen synthesis and bone preservation. Mainly, we observed that 14-3-3ζ down-regulates interleukin (IL)-1β and up-regulates the IL-1 receptor antagonist, thereby causing arthritis suppression. Overall, our results show that 14-3-3ζ is a suppressor of inflammatory arthritis, which might have therapeutic implications in RA.

Results

14-3-3ζ KO Rats Develop Early and Severe PIA. To investigate the role of endogenous 14-3-3ζ protein in the pathogenesis of IA, we generated 14-3-3ζ global KO rats using a CRISPR-Cas9 technology (36). A 58-bp deletion in exon 3 of the 14-3-3ζ gene resulted in global KO in LEW rats (*SI Appendix*, Fig. S1*A*). The KO rats are not good breeders, an observation similar to reports on 14-3-3ζ KO mice (37, 38); therefore, heterozygous animals were used for breeding. Loss of 14-3-3ζ resulted in reduced anti-14-3-3ζ antibody levels in the KO animals. We measured antibody levels at various dilutions of plasma using in-house standardized enzyme-linked immunosorbent assay (ELISA) and observed ∼90% loss of 14-3-3ζ antibody in KO animals compared with WT (*SI Appendix*, Fig. S1*B*). The remaining 10% antibody reflected the nonspecific binding, probably due to a high degree of sequence conservation in 14-3-3 family members (39). To account for 14-3-3ζ specificity in antibody measurements, we subtracted all future ELISA values by 10%. The absence of 14-3-3ζ in the KO animals did not affect 14-3-3η antibodies in the plasma (*SI Appendix*, Fig. S1*C*).

Animal models of IA share several features with human RA, including T-cell dominance (33, 34). The initiation of arthritis in LEW rats resulted in a typical three-phase disease, including an asymptomatic period and severe joint inflammation, followed by a resolution phase in which inflammation starts to subside (*SI Appendix*, Fig. S1*D*) (34, 40). We used a 0 to 80 scoring system of arthritis, as previously published (41). Compared with WT, pristane induced an early-onset joint inflammation with significantly higher arthritic scores in 14-3-3ζ KO animals. The increase in arthritis scores correlated with the decreased weight gain during the experiment (Fig. 1*A*). Compared with WT, the 14-3-3ζ KO animals showed highly inflamed swollen joints, which accounted for higher arthritis scores (Fig. 1*B*). The arthritic ankle and knee joints were studied using micro computed tomography (μCT). The μCT analysis of ankle and knee joints showed that the bones from the 14-3-3ζ KO animals had increased abnormal ectopic bone and significant bone surface damage. The increased bone erosion associated with growth plate and articular surfaces was strikingly prominent in the 14-3-3ζ KO animals. The proximal tibia and femur showed a significant trabecular bone loss in 14-3-3ζ KO rats (Fig. 1*C*).

Histological analyses of ankle and knee joints showed an increased immune cell infiltration in the synovium of 14-3-3ζ KO animals (Fig. 1*D*). There was no significant difference in the 14-3-3ζ antibody levels in the synovial fluid of KO animals compared with WT animals (Fig. 1*E*). The serological cytokine analysis showed no substantial changes in IL-17A or IL-6 in 14-3-3ζ KO animals (Fig. 1 *F* and *G*). To determine if arthritis susceptibility was PIA specific, we examined 14-3-3ζ KO in the CIA model. Like PIA, 14-3-3ζ KO animals developed much higher inflammation of joints resulting in significant arthritis scores (*SI Appendix*, Fig. S1*E*). These results suggest that endogenous 14-3-3ζ has a unique function in the suppression of IA.

14-3-3ζ Antibodies Are Not Responsible for Arthritis Suppression. Higher arthritis scores and reduced 14-3-3ζ antibodies in the KO animals (*SI Appendix*, Fig. S1*B*) made us question if a decrease in 14-3-3ζ antibodies is responsible for severe arthritis. We first examined how the progression of arthritis impacted the levels of 14-3-3ζ antibodies in WT LEW rats. We measured 14-3-3ζ antibodies in the plasma of WT animals injected with pristane

at the onset of symptoms (15 d) and resolution (∼45 d). The level of the 14-3-3ζ antibody significantly decreased by the time experimental arthritis symptoms were visible and remained low for the duration of the study (Fig. 2 *A* and *B*). Arthritis scores and 14-3-3ζ antibody levels were inversely correlated, and their relationship was statistically significant (*SI Appendix*, Fig. S2*A*). This led us to examine a possible protective role of 14-3-3ζ antibodies in IA.

To test the role of the 14-3-3ζ antibody, we performed passive antibody administration by convalescent plasma transfusion to WT and KO animals after arthritis initiation with pristane. We obtained 14-3-3ζ antibody–containing plasma from 18-d post-immunized WT LEW rats. Half of the pooled plasma was processed to remove 14-3-3ζ antibody by incubating with a column-bound purified 14-3-3ζ protein, which resulted in >75% reduction in the antibodies (Fig. 2*C*). Original plasma or one with depleted 14-3-3ζ antibodies was used for the infusion during arthritis progression, per the scheme shown in Fig. 2*C*. At 14, 21, and 28 d postpristane, three intravenous injections of plasma were performed (Fig. 2*C*). Animals were regularly examined for arthritis and body weight. There were no immediate or long-term effects of passive plasma transfer on arthritis progression, as shown in the arthritis scores of WT or 14-3-3ζ KO animals (Fig. 2 *D* and *E*). The 14-3-3ζ antibody levels measured 1 d postinfusion showed restoration of its levels (Fig. 2*F*). Furthermore, regardless of the type of plasma infused, no correlation between serum antibody levels and IA score was observed in WT or KO animals (Fig. 2*G*). Additionally, infusion at earlier time points did not result in arthritis suppression (*SI Appendix*, Fig. S2 *B* and *C*). These results suggest that 14-3-3ζ antibodies do not contribute to the suppression of arthritis.

Immunization with 14-3-3ζ Prevents IA Progression in 14-3-3ζ KO Rats. After ruling out the protective function of antibodies, we questioned if 14-3-3ζ's antigenic role is responsible for arthritis suppression. To test, we performed 14-3-3ζ immunization in the KO animals, since they exhibit severe arthritis in both PIA and CIA models of IA. Animals were divided into two groups; one received purified human 14-3-3ζ mixed with IFA, while the other received only IFA (Fig. 3*A*). A two-dose immunization strategy—the first at 1 d and booster at 8 d postpristane—was adopted, and the effect on the arthritis progression was measured. Compared with IFA alone, immunization with 14-3-3ζ significantly reduced the disease progression, as evidenced by lower arthritic scores in KO animals. Decreased arthritis severity in 14-3-3ζ–treated animals correlated with the increase in weight gain during the study (Fig. 3*B*). Limb swelling was visibly reduced in the animals that received 14-3-3ζ (Fig. 3*C*). The μCT analysis of the tibia bones from 14-3-3ζ KO animals showed a significant loss of trabecular bone and cortical bone thickness in the IFA-treated animals. Importantly, 14-3-3ζ immunization protected both the trabecular bone and cortical bone (Fig. 3*D*).

The histological assessment of the inflamed joints from IFA-treated animals showed a significant infiltration of immune cells. In comparison, 14-3-3ζ–treated animals had reduced immune cells in the joints (Fig. 3*E*), further demonstrating the immune suppression. To verify this observation, we evaluated the effect of 14-3-3ζ immunization in the CIA model. Like PIA, 14-3-3ζ KO in the CIA model showed severely inflamed joints and high arthritis scores, which were significantly reduced in animals immunized with 14-3-3ζ (*SI Appendix*, Fig. S3*A*).

To examine the immunogenic function, we measured how 14-3-3ζ treatment affects cytokine and antibody induction in vivo. The 14-3-3ζ immunization resulted in a significant increase of plasma antibody and IL-17A but not in IL-6 (Fig. 3 *F–H*). Similar to plasma, 14-3-3ζ antibody levels in the synovial fluid of the 14-3-3ζ–immunized animals were also increased (Fig. 3*I*). In comparison with >300-fold induction in the 14-3-3ζ antibody in WT,
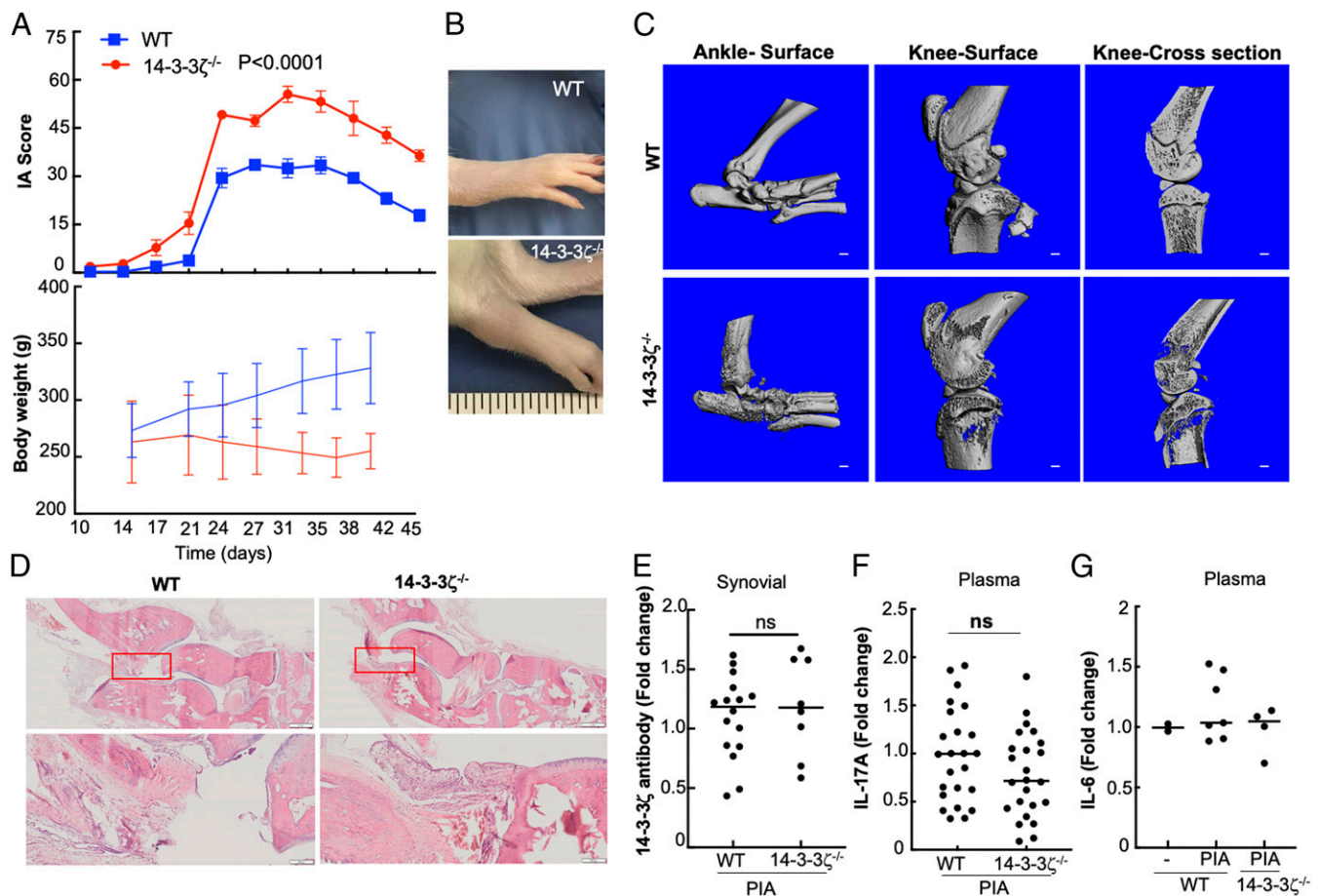
www.manaraa.com

Fig. 1. 14-3-3ζ KO rats exhibit severe and early IA. (*A*) The WT (*n* = 8) and KO animals (*n* = 8) were subjected to PIA. The experiment was repeated at least three times. Representative body weight gain and IA score during PIA are shown. (*B*) Representative pictures showing inflamed joint in WT versus KO animals are shown. (*C*) The 3D reconstruction of μCT scans of ankle and knee joints are shown. (Scale bar: 1 mm.) (*D*) Hematoxylin and eosin (H&E) staining of ankles harvested from WT or 14-3-3ζ KO rats were compared for bone damage and infiltrating immune cells. (Scale bar: 200 μm.) (*E*) The 14-3-3ζ antibody levels in synovial fluid were measured in WT and KO animals using ELISA. (*F* and *G*) Plasma profile of IL-17A and IL-6 measured in WT and KO animals using ELISA.

the effect on 14-3-3η antibody was marginal (*SI Appendix*, Fig. S3B). To examine side effects of 14-3-3ζ immunogenicity, we subjected LEW rats to two doses of immunization with IFA alone or with 14-3-3ζ. In the absence of pristane, 14-3-3ζ immunization or IFA alone had minimal effect on joint inflammation or any other physical symptoms (*SI Appendix*, Fig. S3C). Since IL-17A increase is associated with RA (32, 42, 43), we examined if a 14-3-3ζ–stimulated IL-17A increase is sufficient to cause arthritis. We subjected Wistar rats to pristane and the immunization strategy, as shown in Fig. 3A. Like LEW rats, 14-3-3ζ immunization of Wistar rats resulted in the significant antibody and IL-17A induction but no significant change in the arthritic score (*SI Appendix*, Fig. S3D). Overall, these results show that in vivo antigenic function of 14-3-3ζ prevents inflammatory arthritis in the LEW rat model of PIA and CIA.

14-3-3ζ Immunization Suppresses Arthritis in WT LEW Rats. We used WT LEW animals to examine the effect of 14-3-3ζ–mediated IA suppression on mild arthritic disease. The IFA-treated WT LEW rats showed a significant increase in joint inflammation by 28 d postpristane injection, which remained high until the end of the experiment at 45 d. Comparatively, the animals immunized with IFA plus 14-3-3ζ showed a substantial reduction in arthritis scores. No significant difference in body weight was observed between the two groups (Fig. 4A). Visually, 14-3-3ζ–immunized animals had less swollen joints (Fig. 4B). Like KO, 14-3-3ζ immunization

induced robust antibody production as measured in the plasma and synovial fluid of the arthritic WT animals (Fig. 4 *C* and *D*). A significant increase in the IL-17A level was observed in 14-3-3ζ–immunized rats (Fig. 4E).

Histological analyses of affected ankles showed significant damage to the synovium, and inflammatory cell infiltrates in the joints of IFA-treated rats, compared with animals that were immunized with 14-3-3ζ (Fig. 4F). The μCT analysis of the tibia also confirmed improvement in the trabecular bone and cortical bone thickness upon 14-3-3ζ immunization (Fig. 4G). These results confirmed that 14-3-3ζ immunization reduces immune cell infiltration in the synovium and improves arthritis scores in rats.

14-3-3ζ Prevents Bone Damage. The findings of 14-3-3ζ immunization–based improvements in trabecular and cortical bone in the KO and WT animals prompted us to investigate how 14-3-3ζ affects the overall bone quality. The μCT analysis of arthritic WT and KO bones revealed that the 14-3-3ζ loss resulted in the decreased cortical bone area, tissue mineral density, cortical bone thickness, trabecular bone/total bone volume ratio, connectivity density, and trabecular thickness (Fig. 5 *A–G*). Marrow area and trabecular separation were increased in the proximal tibia (Fig. 5H). While most of these parameters were improved in the bones obtained from 14-3-3ζ–immunized WT and KO animals, the most significant improvements were observed in the parameters including tissue mineral density, trabecular bone/total bone volume ratio,
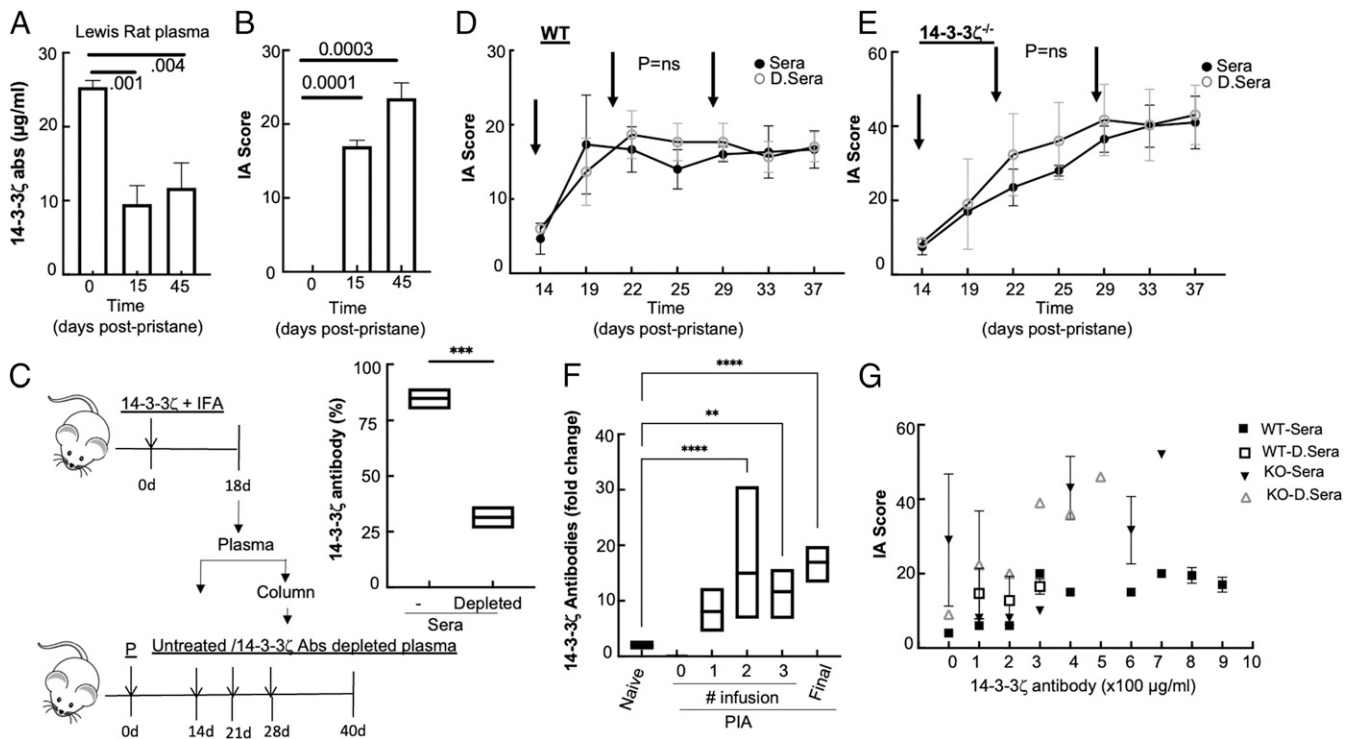
www.manaraa.com

Fig. 2. 14-3-3ζ antibodies are not responsible for IA suppression. (*A*) The 14-3-3ζ antibody level was measured in the plasma of WT LEW rats using the in-house standardized ELISA method. (*B*) Corresponding IA scores at the time of plasma collection are shown. (*C*) A schematic of generating plasma and use for passive immunization is shown. The percent decrease in the plasma 14-3-3ζ antibodies after the incubating with GST-bound 14-3-3ζ beads was measured using ELISA. (*D* and *E*) The 200 μL complete or 14-3-3ζ antibody–depleted plasma was intravenously injected into the tail vein of WT (*D*, n = 6) or KO (*E*, n = 6) LEW rats. Arrows indicate the time of infusion after the pristane injection. Animals were monitored over a period of 40 d. RA scores were measured twice a week. (*F*) Fold change in 14-3-3ζ antibody level in sera after 1 d postinfusion was measured using ELISA. (*G*) IA scores were plotted against the sera 14-3-3ζ antibody levels (at the interval of 100 μg/mL) of WT and KO animals infused with complete or depleted plasma. **$P < 0.005$, ***$P < 0.0005$, and ****$P < 0.0001$.

and connectivity density (Fig. 5 *C*, *E*, and *F*). Increased trabecular bone mass and trabeculae resulted in decreased trabecular separation by 14-3-3ζ immunization, further strengthening its direct impact on bone health (Fig. 5*H*).

14-3-3ζ Promotes Collagen Expression. The observation of loss of tissue mineral density and trabecular bone triggered us to examine how 14-3-3ζ affects collagen level. Compared with WT, collagen staining in the naïve KO animals was reduced. Induction of IA resulted in further loss of collagen levels in both WT and KO tibia (Fig. 6*A*). Collagen expression levels were restored upon 14-3-3ζ treatment (Fig. 6*A*). Similar to the overall bone, the collagen content of WT and KO trabecular bones was also significantly improved by 14-3-3ζ (Fig. 6*B*). To confirm the effect on collagen levels, we studied primary rat bone marrow–derived mesenchymal cells that were cultured in osteoblast differentiating media in the presence of recombinant 14-3-3ζ protein purified from human embryonic kidney (HEK)293T cells (*SI Appendix,* Fig. S4*A*). In the presence of 14-3-3ζ, rat mesenchymal cells showed a dose-dependent increase in collagen 1 transcripts without significant impact on cell growth (Fig. 6*C* and *SI Appendix,* Fig. S4*B*). Increased collagen 1 messenger RNA (mRNA) levels were also observed in mesenchymal cells isolated from 14-3-3ζ KO rats when treated with purified protein (Fig. 6*D*). These findings show that 14-3-3ζ promotes collagen induction in both in vivo and ex vivo models.

14-3-3ζ Suppresses the IL-1β–Signaling Molecules. To investigate the molecular mechanism behind the IA-suppressive role of 14-3-3ζ, we examined the immunological changes in naïve and arthritic

14-3-3ζ KO rats. Compared with WT rats, circulating peripheral blood mononuclear cells (PBMCs) of KO rats showed significantly higher *Il1b* and *Ifng* but insignificant change in *Tnfa* (Fig. 7*A*). Expression of *Il17a* or *Il10* was undetectable in the KO animals. Because IL-1β signaling plays a key role in RA pathogenesis (44), we focused on this cytokine in subsequent studies. As observed in PBMCs, *Il1b* mRNA was also significantly elevated in the bone marrow of 14-3-3ζ KO rats (Fig. 7*B*). Next, we examined whether a similar increase in *Il1b* also occurred during IA. Upon PIA induction, compared with WT, the *Il1b* expression was higher in peripheral and bone marrow cells of 14-3-3ζ KO rats (Fig. 7 *C* and *D*). Furthermore, KO PBMCs also showed a significant increase in the tartrate-resistant acid phosphatase (*Trap*) expression, but not in osteoprotegerin (*Opg*), suggesting that osteoclast activation may be responsible for the bone loss observed in the 14-3-3ζ KO rats (Fig. 7*C*).

Next, we examined the effect of 14-3-3ζ immunization on *Il1b* expression in the PIA model. PBMCs, collected from 14-3-3ζ–immunized animals after 1 wk of immunization, showed a significant reduction in *Il1b* compared with animals treated with IFA only (Fig. 7*E*). In contrast, the IL-1 receptor antagonist (*Il1rn*) expression level was elevated in the 14-3-3ζ–treated rats (Fig. 7*E*). Compared with the WT, the IL-1β protein was increased in naïve as well as pristane-treated 14-3-3ζ KO rats (Fig. 7*F*). The 14-3-3ζ treatment led to reduced levels of circulating IL-1β protein levels in both WT and KO rats (Fig. 7*F*). Expression of other proinflammatory cytokines, including *Cxcl1*, *Ifng*, and *Tnfa*, was also reduced in the 14-3-3ζ–immunized animals (*SI Appendix,* Fig. S5 *A*–*C*).

Collectively, we show that 14-3-3ζ causes immune suppression by interfering with the IL-1β pathway, as well as bone remodeling
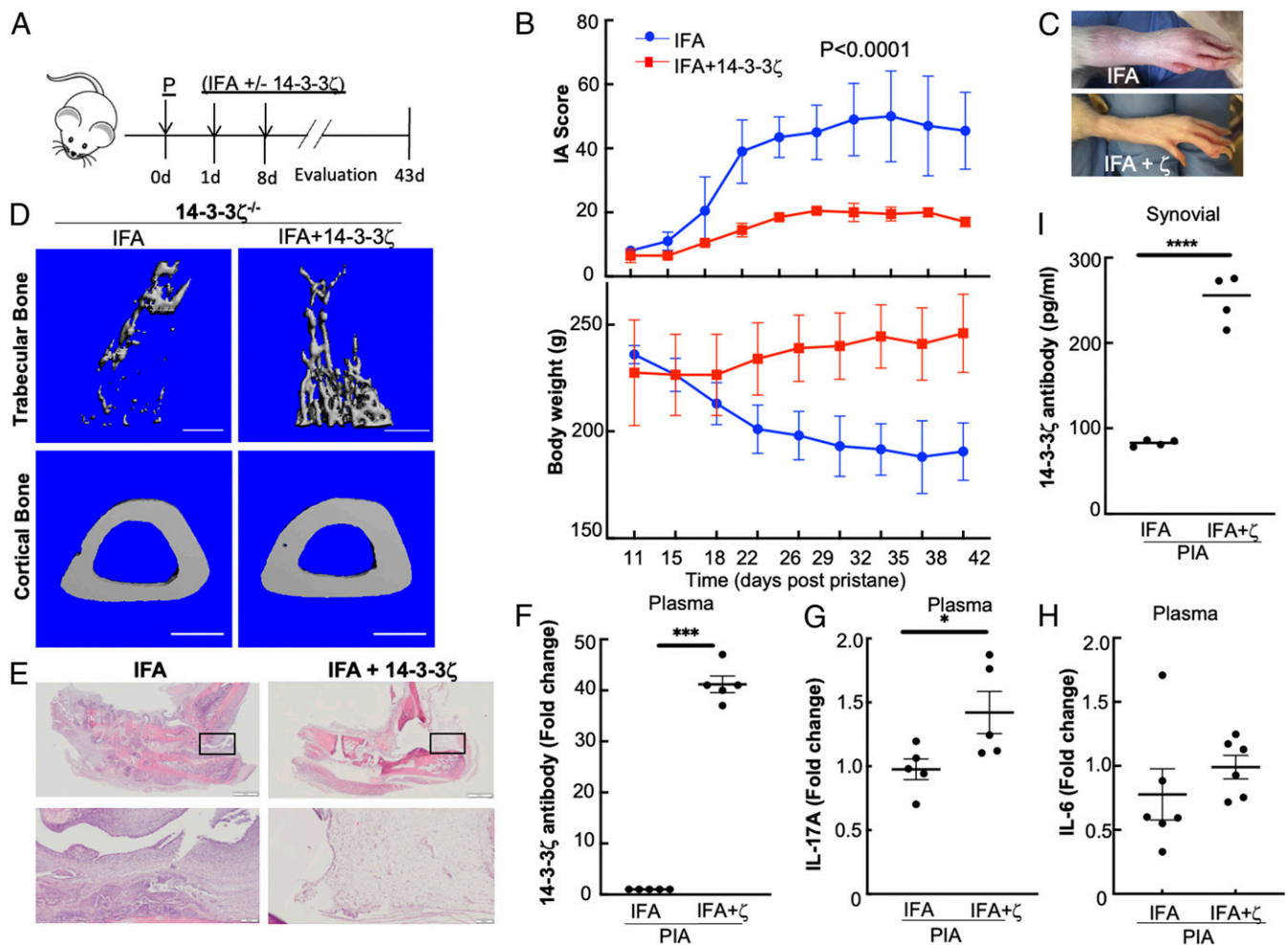
www.manaraa.com

Fig. 3. Immunization with 14-3-3ζ in KO rats rescues the IA suppression. (*A*) Experimental design of 14-3-3ζ immunization in the PIA model using 8-wk-old LEW rats is shown. The 150 μL IFA either alone or mixed with 14-3-3ζ was injected at 1 d and 8 d postpristane (P). (*B*) The effect of 14-3-3ζ immunization on body weight and IA scores in 14-3-3ζ KO (*n* = 5) rats were compared. The experiment was repeated at least three times; a representative experiment is shown. (*C*) Representative pictures of the inflamed joint in 14-3-3ζ KO rats treated with IFA or 14-3-3ζ are shown. (*D*) The 3D reconstructions of μCT images from IFA- or IFA plus 14-3-3ζ–treated animals were constructed to show recovery of the trabecular bone or cortical bone thickness upon immunization. (Scale bar: 1 mm.) (*E*) The H&E stain of inflamed ankles of 14-3-3ζ KO rats shows that immunization with 14-3-3ζ suppresses the infiltration of immune cells in the joints. (Scale bar: 2 mm.) The inset is shown in the lower lane. (Scale bar: 200 μm.) (*F–H*) The plasma levels of 14-3-3ζ antibody (*F*), IL-17A (*G*), and IL-6 (*H*) at the end of the study were measured using ELISA. (*I*) The 14-3-3ζ antibody level in the synovial fluid was measured using the in-house standardized ELISA. *$P < 0.05$, ***$P < 0.0005$, and ****$P < 0.0001$.

by promoting collagen synthesis, and functions as an endogenous suppressor of IA in vivo (Fig. 7*G*).

Discussion

The 14-3-3ζ protein is a vital adaptor protein regulating several cellular processes including immune responses (26, 45, 46). Our study shows that 14-3-3ζ has an arthritis-suppressive function in LEW rats. Global 14-3-3ζ KO rats show increased susceptibility to arthritis in both PIA and CIA models, providing strong evidence of the arthritis-suppressive role by an endogenous protein. The arthritic 14-3-3ζ KO animals showed increased bone surface damage with abnormal ectopic bone formation in the ankle and knee joints. Severe bone erosion in the growth plate and articular surfaces was observed in the knee joints and femoral heads of 14-3-3ζ KO rats. The 14-3-3ζ KO bones, including the femur and tibia (distal and proximal), showed a severe trabecular bone loss compared with the WT animals. Histological analyses confirmed the increased bone damage and synovial inflammation in 14-3-3ζ KO animals. The 14-3-3ζ immunization in both WT and 14-3-3ζ KO LEW rats protected animals from arthritis in both PIA and

CIA models. Notably, the 14-3-3ζ immunization improved the collagen content, tissue mineral density, and trabecular bone volume. The improvement in joint inflammation was mirrored by a decrease in several proinflammatory cytokine productions, including *Il1b*, *Cxcl1*, *Ifng*, and *Tnfa*. Time-course analysis showing up-regulation of *Il1rn* coupled with a decrease in *Il1b* post-14-3-3ζ immunization might explain immune suppression caused by 14-3-3ζ. It is important to note that 14-3-3ζ inhibition of pyrin-dependent inflammasome activation has been previously reported (47). There were no visual or arthritic symptoms when animals were immunized with 14-3-3ζ in the absence of pristane. Similarly, increase in 14-3-3ζ antibody and IL-17A was not sufficient for induction of IA in Wistar rats that show resistance to arthritis (48). Therefore, we conclude that 14-3-3ζ has a suppressive effect on IA, which does not depend upon antibody level; instead, it requires active immunogenic function via suppression of IL-1β and promotion of collagen synthesis (Fig. 7*G*).

The PIA model is strongly affected by age but not by biological sex or housing environment (34). Pristane-induced cell death generates autoantigens recognized by major histocompatibility
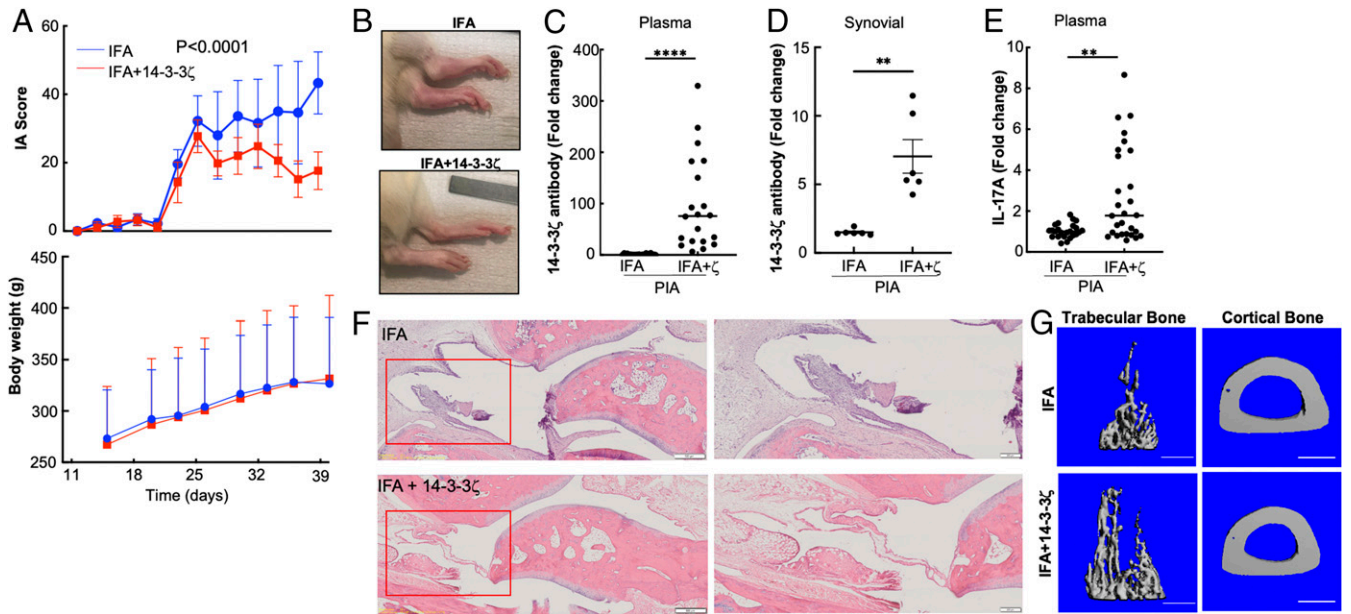
Fig. 4. Immunization with 14-3-3ζ suppresses IA in WT LEW rats. (*A*) The 8-wk-old WT LEW rats were subjected to PIA followed by injection with IFA alone or mixed with 14-3-3ζ protein, as shown in Fig 3*A*. Animals were monitored for body weight and arthritis scores (*n* = 4). The experiment was repeated at least three times; a representative experiment is shown. (*B*) Representative pictures of inflamed joints are shown. (*C* and *D*) The 14-3-3ζ antibody level in the plasma (*C*) and synovial fluid (*D*) was measured using standardized ELISA. (*E*) The plasma IL-17A level in the IFA-treated versus IFA+14-3-3ζ–treated animals was measured using ELISA. (*F*) The H&E staining shows an effect of 14-3-3ζ immunization on the immune cell infiltration in the ankle joint. (Scale bar: 500 μm.) The magnified image of the inset is shown on the right. (Scale bar: 200 μm.) (*G*) The 3D reconstructions of IFA- and IFA+14-3-3ζ–treated animals show the effect of 14-3-3ζ immunization on the trabecular bone and cortical bone thickness. Scale bar: 1 mm. **P < 0.005, and ****P < 0.0001.

complex (MHC) class II–restricted arthritogenic T cells responsible for arthritis development (33, 49). We recently showed that exogenous 14-3-3ζ promotes Th1 and Th17 cell polarization in human PBMC and cytokine (IFN-γ and IL-17A) production (32). Consistent with our previous ex vivo findings, here, we observed that 14-3-3ζ immunization resulted in robust antibody
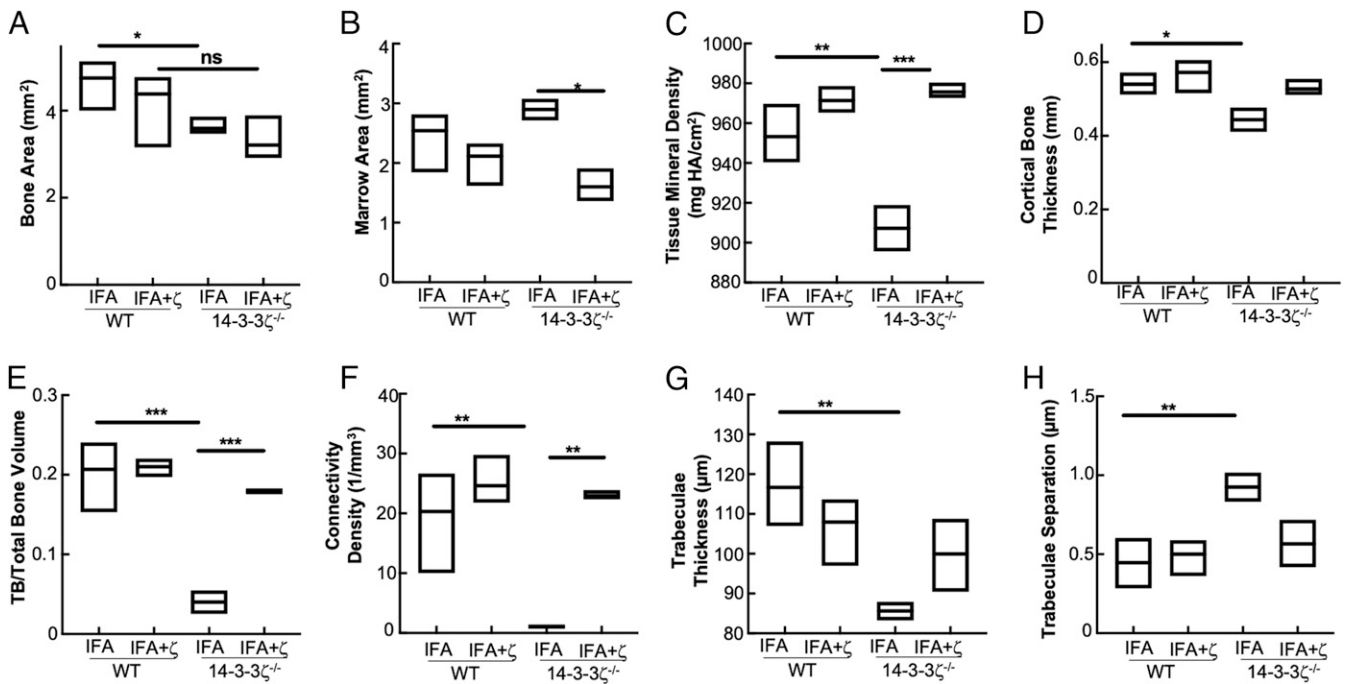

Fig. 5. 14-3-3ζ promotes cortical and trabecular bone development. The μCT analysis was used to study the effect of 14-3-3ζ in gene KO and immunized animals. Bones from arthritic WT and 14-3-3ζ KO rats (*n* = 4) were analyzed to make the measurements of (*A*) bone area, (*B*) marrow area, (*C*) tissue mineral density, (*D*) cortical bone thickness, (*E*) ratio of trabecular versus total bone volume, (*F*) connectivity density, (*G*) trabecular thickness, and (*H*) trabecular separation. *P < 0.05, **P < 0.005, and ***P < 0.0005.
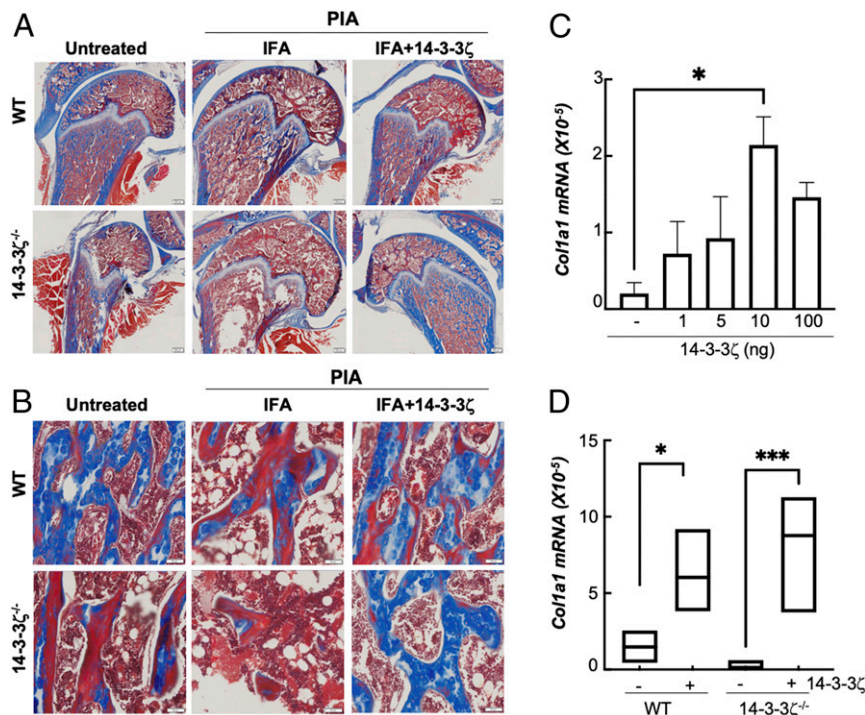
Fig. 6. 14-3-3ζ promotes collagen synthesis. (*A* and *B*) Tibia (*A*) and trabecular bones (*B*) from WT and 14-3-3ζ KO–untreated, IFA-, and IFA+14-3-3ζ–treated arthritic animals were stained for collagen with mason trichrome. (Scale bar: 500 μm and 50 μm for *A* and *B*, respectively.) (*C*) Primary rat mesenchymal cells were treated with different amounts of purified recombinant His-14-3-3ζ protein for 14 d, and the effect on collagen1 gene induction was measured using RT-qPCR. (*D*) Primary rat mesenchymal cells from WT and KO cells were treated with 100 ng recombinant His-14-3-3ζ for 14 d, and collagen1 gene induction was measured using RT-qPCR. *$P < 0.05$, and ***$P < 0.0005$.

and significant IL-17A production but not IL-6. We previously showed 14-3-3ζ is required for IL-17A–stimulated IL-6 levels but not Cxcl-1 that may influence inflammation (36). It is also noteworthy that IFN-γ levels, but not IL-17A or IL-6, drive arthritis in the PIA rat model (49–52). The decrease in IL-1β, IFN-γ, and tumor necrosis factor (TNF)-α mRNA levels by 14-3-3ζ immunization could explain improved bone health and low arthritis scores (33, 53, 54). The 14-3-3ζ–mediated immune suppression did not involve IL-10; however, we observed that 14-3-3ζ KO and IL-1R2 KO animals share several common features including increased arthritis susceptibility independent of T-cell and antibody responses (55). It is well documented that higher plasma and synovial IL-1β levels in RA contribute to the increased prostaglandin E2, matrix metalloproteases, and bone damage (44). IL-1β signaling requires IL-1R1, which is competitively inhibited by IL-1R2 and IL-1RA (*IL1RN* gene) (44). It is worth mentioning that IL-1RA inhibition is successfully used for treating RA (56). How 14-3-3ζ suppresses *Il1b* levels or promotes *Il1rn* remains an interesting question for future studies.

A better understanding of IA's immune mechanisms has led to improved treatments, including cytokine blockers and other biologic therapies (57). However, the role of autoantigens (peptidyl arginine deiminase 4, glucose-6-phosphate isomerase, heat shock proteins, and heterogeneous nuclear ribonucleoprotein, etc.) in IA pathogenesis remains unclear (10, 58). It is important to mention that a few other autoantigens, including immunoglobulin-binding protein and DNAjp, have shown therapeutic potential in RA treatment by promoting anti-inflammatory responses (16, 59). Unlike autoantigens, rheumatoid factor and anticitrullinated cyclic peptide antibodies associate with severe disease (60–64). In contrast, we show that 14-3-3ζ antibodies decrease upon IA induction. Unlike other diseases (6, 65), passive immunization with 14-3-3ζ antibodies did not affect IA pathogenesis. While the role of 14-3-3ζ antibodies remains debatable, their presence in healthy sera

confirms the immunogenic nature of endogenous 14-3-3ζ in humans (66).

While 14-3-3ζ is predominantly intracellular, several reports of its extracellular presence and function are published (29, 67). In RA, activated B cells show reduced 14-3-3ζ peptide secretion (68). The basis of 14-3-3ζ antibody loss we observed in arthritic animals can be explained by either a decreased level of antigenic peptide or loss of antigenicity. One study recently showed the presence of extracellular 14-3-3ζ in the sera of arthritic mice and urine of RA patients, and it is a primary secretory factor responsible for the resolution of arthritis in mice (69). Unlike the systemic effects observed in our study, Kong et al. noticed local inflammation suppression upon increasing 14-3-3ζ using adenoviral constructs directly to the joints (69). These reports further support our conclusion that 14-3-3ζ has a key role in arthritis and immune suppression. This finding raises many challenging questions related to 14-3-3ζ's role in other immune dysfunction and musculoskeletal abnormalities (70, 71). We expect that 14-3-3ζ will become a valuable tool in the prevention and treatment of IA.

In summary, we show here that 14-3-3ζ is an immunogen with a function of inflammatory arthritis suppression. These results suggest that the 14-3-3ζ participates in an endogenous host-protective anti-arthritis immune mechanism, which deserves further investigation.

Methods

Purification of 14-3-3ζ Protein. The previously described protocol for 14-3-3ζ purification was utilized (32). Briefly, the BL-21 strain of *Escherichia coli*
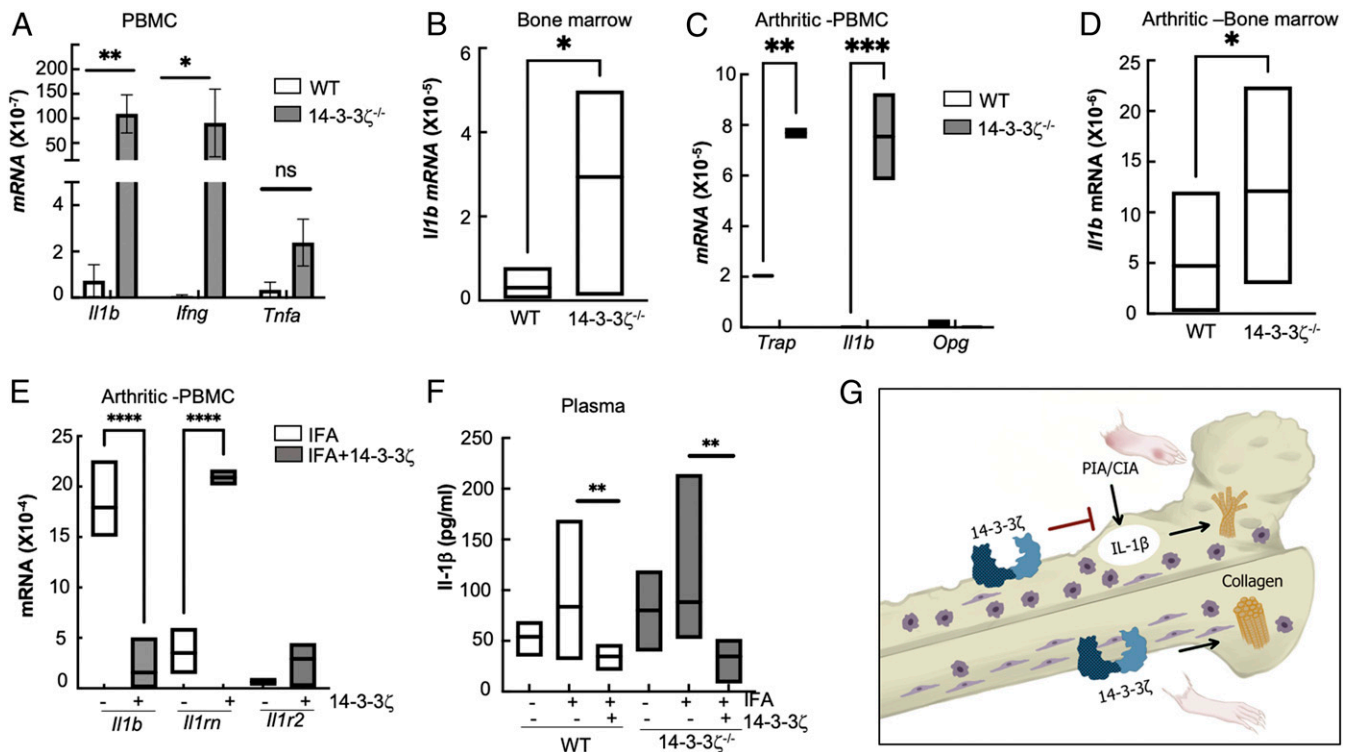
IMMUNOLOGY AND INFLAMMATION

Fig. 7. 14-3-3ζ supplementation interferes with IL-1β signaling. (*A*) Expression of proinflammatory cytokines, including *Il1b*, *Ifng*, and *Tnfa*, was measured in the circulating immune cells of WT and 14-3-3ζ KO–naïve animals using RT-qPCR. (*B*) The *Il1b* transcript in the bone marrow of naïve 14-3-3ζ KO as compared with WT using RT-qPCR. (*C*) Expression of *Il1b*, *Trap*, and *Opg*, was measured in the circulating immune cells of WT and 14-3-3ζ KO arthritic animals using RT-qPCR. (*D*) The *Il1b* transcript in the bone marrow of arthritic 14-3-3ζ KO as compared with WT animals using RT-qPCR. (*E*) Expression in PBMC of 1 wk postimmunization in the 14-3-3ζ KO animals that received IFA alone or with 14-3-3ζ protein. (*F*) IL-1β was measured in the plasma of WT and KO–naïve or arthritic animals using quantitative ELISA. (*G*) Overall model depicts that the absence of 14-3-3ζ results in severe inflammation and bone damage; mainly, increased IL-1β and reduced collagen levels are observed in the naïve and IA-affected animals. Immunization with 14-3-3ζ interferes with IL-1β and promotes collagen synthesis to prevent inflammation and bone damage. $*P < 0.05$, $**P < 0.005$, $***P < 0.0005$, and $****P < 0.0001$.

expressing GST-14-3-3ζ was grown and induced by 1 mM IPTG for 24 h. Bacteria were centrifuged and lysed by sonication. GST beads were used to pull down tagged 14-3-3ζ, which was eluted from the resin with 10 mM glutathione in 100 mM Tris·HCl (pH 8). Eluate was concentrated using an Amicon 30 K concentrator, then the GST tag was cleaved with thrombin (10 units/mg) for 2 h at 37 °C. The cleaved tag was removed by incubating with fresh equilibrated GST resin for 1.5 h. The protein was then run through an endotoxin-removing spin column after incubating for at least 2 h. Both Coomassie staining and Western blot assessed protein purity after running sodium dodecyl sulfate–polyacrylamide gel electrophoresis. The his-tagged 14-3-3ζ was purified using Ni beads and cell lysates of HEK293T cells over-expressing recombinant protein. Imidazole-based elution followed by concentration and removal of imidazole was performed as per the recommended protocol.

PIA. The 14-3-3ζ KO animals were generated as described before (36). Both WT and KO rats were maintained in the University of Toledo College of Medicine and Life Sciences vivarium and fed a standard diet. All animal experiments were conducted as per approved protocols by the Institutional Animal Care and Use Committee of the University of Toledo. Arthritis was induced in 8- to 10-wk-old male and female LEW rats by anesthetizing with 2% isoflurane in oxygen followed by intradermal injection of 200 μL pristane at the base of the tail. At days 1 and 7 postpristane, either 100 μL IFA or a 1:1 ratio of IFA and purified 14-3-3ζ protein (1 mg/kg) was injected about 2 cm from the initial injection site. Animals were scored for arthritis twice every week unless specified otherwise. For scoring, a system of 0 to 80 with a max score of 20 possible for each limb was followed (35). Each joint of the foot was scored 0 (swelling absent) or 1 (swelling present). Swelling in the wrist, midforepaw, ankle, and midfoot was scored from 0 to 4. Body weight was measured once every week. At the end of the experiment, animals were killed, and body tissues, plasma, and synovial fluid were collected. For synovial fluid, 50 μL sterile phosphate buffered saline (PBS) was injected into the joint cavity. During the experiment, blood was collected at 15 d by

saphenous vein bleeding into ethylenediaminetetraacetic acid (EDTA)-coated tubes.

Plasma Infusion. Age 8- to 11-wk-old WT LEW rats, male and female, were injected with purified 14-3-3ζ protein (1 mg/kg) with IFA as an adjuvant. After 18 d, the rats were killed, and blood was collected in heparin-coated tubes. Half of the plasma obtained was incubated with 14-3-3ζ–bound GST beads (Pierce) overnight to remove 14-3-3ζ antibodies from the plasma. The depletion of 14-3-3ζ antibody in the plasma was confirmed by using ELISA. The 200 μL untreated or depleted plasma was intravenously injected through the tail vein.

Mesenchymal Cell Culture. Cleaned bones from WT and 14-3-3ζ KO rats were collected and washed with sterile PBS. Marrow was collected by spinning it in a clean tube at 1,000 rpm for 5 min. The red blood cells cells were lysed using ammonium-chloride-potassium (ACK) lysis buffer, followed by plating in the Roswell Park Memorial Institute medium containing 15% fetal bovine serum, 0.2 mM ascorbic acid, and 10 mM b-glycerophosphate. After 2 d, nonadherent cells were removed, and the rest of the cells were cultured in the growth media containing dexamethasone until confluent (72).

ELISA. Cytokines (IL-1β, IL-6, IL-17A, and TNF-α) were measured by using the commercial kits and protocols provided by the manufacturer (PeproTech Inc. and R&D Inc.). The 14-3-3ζ antibodies were measured using in-house ELISA. Briefly, the Immobilin 2B plates were coated with purified 14-3-3ζ at 50 ng/mL overnight at 4 °C. Plates were blocked with 1% bovine serum albumin solution for 1 h at room temperature. Rat plasma samples were diluted in sterile PBS (7500× for IFA + 14-3-3ζ–treated, 125× for IFA alone–treated). Diluted rat plasma in triplicate or synovial fluid were directly added to coated wells and incubated on a shaker for 2 h at room temperature (25 °C). After three washing steps in Tris-buffered saline (TBS)-Tween buffer for 5 min each, anti-rat-horseradish peroxidase diluted in TBS-Tween at 1:3,000 was added and incubated on a shaker for 1 h at room temperature. The

Kim et al.
14-3-3ζ: A suppressor of inflammatory arthritis

www.manaraa.com

plate was washed three times, 3,3′,5,5′-Tetramethylbenzidine was added, and the development of color was observed. The reaction was stopped using 2N HCl, and the plate was read at 450 nm using a microplate reader. The absorbance of the control wells, including blank or no plasma controls, was used for subtraction. Commercial antibody at the 0- to 100-ng concentrations was used for the standard equation.

Histology. Both knee and ankle joints were harvested from the killed rats and were cleaned of excess tissue. All samples were initially preserved in 10% neutral buffered formalin fixatives for 2 wk, followed by decalcification in acidified EDTA solution for 5 d. The bones were curetted by the Leica CM3050S (Leica Microsystems AG). All samples were sectioned in the vertical axis, cut at 5-μm thickness, and stained with hematoxylin and eosin or mason trichrome at the University of Toledo imaging core facility. All images were obtained with Olympus VS120-S6-W.

μCT Imaging. Three-dimensional (3D) images of the proximal femur, knee joint, and ankle joint were acquired by μCT using the μCT 35 system (Scanco Medical AG) and using undivided hind leg specimens. Bone scans were performed with the X-ray source operating at 70-kVp and 40-μA energy settings and recording 500 projections/180° acquired at a 300-ms integration time using a 20-μm nominal resolution voxel for all bone locations. Scans encompassing regions of interest were segmented at an optimized lower threshold value of 170 units per mille scale (the equivalent of 2,055 Hounsfield units or linear attenuation coefficient [μ] of 1.36) and with a Gauss filter set to sigma 0.8 and support 1.0. These settings accommodated significant differences in radiodensity within regions of interest and provided an optimized view of the specimens by minimizing image erosion and image overrepresentation in KO and in WT bones, respectively. The 3D renderings of bone specimens were generated using μCT Ray version 4.0-4 software (Scanco Medical AG) with longitudinal sections recorded at ∼50% of the specimen depth.

RNA Isolation and qRT-PCR Analyses. Total RNA was isolated using TRIzol (Invitrogen), complementary DNA (cDNA) was prepared using the ImProm-II Reverse Transcription Kit (Promega), and the cDNA was analyzed using Radiant SYBR Green PCR mix (Alkali Scientific Inc.) in the Roche LightCycler 96 instrument and analyzed with the LightCycler 480 Software, version 1.5. The expression levels of the mRNAs were normalized to 18S ribosomal RNA. For the qRT-PCR analyses of the respective genes, the following primers were used (73):

Cxcl-1: GGATTCACCTCAAGAACATCCAGA

CACCCTTCTACTAGCACAGTGGTTG

Il-10: TGCCAAGCCTTGTCAGAAATGATCAAG

GTATCCAGAGGGTCTTCAGCTTCTCTC

Tnf-α: ACC ACG CTC TTC TGT CTA CTG

CTT GGT GGT TTG CTA CGA C

Ifn-γ: ATGAGTGCTACACGCCGCGTCTTGG

GAGTTCATTGACAGCTTTGTGCTGG

Il-1b: GCAATGGTCGGGACATAGTT

AGACCTGACTTGGCAGAGGA

Il-1rn: AAGACCTTCTACCTGAGGAACAACC

GCCCAAGAACACATTCCGAAAGTC

Il-r2: CATTCAGACACCTCCAGCAGTTC

ACCCAGAGCGTATCATCCTTCAC

Il-17A: CTTCACCCTGGACTCTGAGC

ATCTTCTCCACCCGGAAAGT

Statistical Analysis. All experiments were performed at least thrice unless stated otherwise. Depending upon the number of sets for comparison, either an unpaired Student's t test or one-way ANOVA was used. $P < 0.05$ was used for statistical significance.

Data Availability. All study data are included in the article and/or *SI Appendix*.

1. A. Gierut, H. Perlman, R. M. Pope, Innate immunity and rheumatoid arthritis. *Rheum. Dis. Clin. North Am.* **36**, 271–296 (2010).
2. I. B. McInnes, G. Schett, Cytokines in the pathogenesis of rheumatoid arthritis. *Nat. Rev. Immunol.* **7**, 429–442 (2007).
3. V. Malmström, A. I. Catrina, L. Klareskog, The immunopathogenesis of seropositive rheumatoid arthritis: From triggering to targeting. *Nat. Rev. Immunol.* **17**, 60–75 (2017).
4. Z. Szekanecz, J. Kim, A. E. Koch, Chemokines and chemokine receptors in rheumatoid arthritis. *Semin. Immunol.* **15**, 15–21 (2003).
5. G. Cambridge et al., Serologic changes following B lymphocyte depletion therapy for rheumatoid arthritis. *Arthritis Rheum.* **48**, 2146–2154 (2003).
6. G. Wildbaum, M. A. Nahir, N. Karin, Beneficial autoimmunity to proinflammatory mediators restrains the consequences of self-destructive immunity. *Immunity* **19**, 679–688 (2003).
7. G. J. Silverman, J. Vas, C. Grönwall, Protective autoantibodies in the rheumatic diseases: Lessons for therapy. *Nat. Rev. Rheumatol.* **9**, 291–300 (2013).
8. Y. Chen et al., Regulation of dendritic cells and macrophages by an anti-apoptotic cell natural antibody that suppresses TLR responses and inhibits inflammatory arthritis. *J. Immunol.* **183**, 1346–1359 (2009).
9. A. E. Morelli et al., Internalization of circulating apoptotic cells by splenic marginal zone dendritic cells: Dependence on complement receptors and effect on cytokine production. *Blood* **101**, 611–620 (2003).
10. V. M. Corrigall, G. S. Panayi, Autoantigens and immune pathways in rheumatoid arthritis. *Crit. Rev. Immunol.* **22**, 281–293 (2002).
11. E. Corsiero, F. Pratesi, E. Prediletto, M. Bombardieri, P. Migliorini, NETosis as source of autoantigens in rheumatoid arthritis. *Front. Immunol.* **7**, 485 (2016).
12. P. J. Utz, T. J. Gensler, P. Anderson, Death, autoantigen modifications, and tolerance. *Arthritis Res.* **2**, 101–114 (2000).
13. E. Darrah, F. Andrade, NETs: The missing link between cell death and systemic autoimmune diseases? *Front. Immunol.* **3**, 428 (2013).
14. F. Zhang et al., Defining inflammatory cell states in rheumatoid arthritis joint synovial tissues by integrating single-cell transcriptomics and mass cytometry. *Nat. Immunol.* **20**, 928–942 (2019).
15. L. Steinman, P. P. Ho, W. H. Robinson, P. J. Utz, P. Villoslada, Antigen-specific tolerance to self-antigens in protein replacement therapy, gene therapy and autoimmunity. *Curr. Opin. Immunol.* **61**, 46–53 (2019).
16. T. E. Ichim et al., Antigen-specific therapy of rheumatoid arthritis. *Expert Opin. Biol. Ther.* **8**, 191–199 (2008).
17. R. Thomas, Dendritic cells and the promise of antigen-specific therapy in rheumatoid arthritis. *Arthritis Res. Ther.* **15**, 204 (2013).
18. T. T. Cheung, I. B. McInnes, Future therapeutic targets in rheumatoid arthritis? *Semin. Immunopathol.* **39**, 487–500 (2017).
19. N. N. Sluchanko, N. B. Gusev, Moonlighting chaperone-like activity of the universal regulatory 14-3-3 proteins. *FEBS J.* **284**, 1279–1295 (2017).
20. K. Funami, M. Matsumoto, C. Obuse, T. Seya, 14-3-3-zeta participates in TLR3-mediated TICAM-1 signal-platform formation. *Mol. Immunol.* **73**, 60–68 (2016).
21. V. K. Weerasekara et al., Metabolic-stress-induced rearrangement of the 14-3-3ζ interactome promotes autophagy via a ULK1- and AMPK-regulated 14-3-3ζ interaction with phosphorylated Atg9. *Mol. Cell. Biol.* **34**, 4379–4388 (2014).
22. D. Thomas, M. Guthridge, J. Woodcock, A. Lopez, 14-3-3 protein signaling in development and growth factor responses. *Curr. Top. Dev. Biol.* **67**, 285–303 (2005).
23. C. L. Neal, D. Yu, 14-3-3ζ as a prognostic marker and therapeutic target for cancer. *Expert Opin. Ther. Targets* **14**, 1343–1354 (2010).
24. I. K. Popov et al., A YWHAZ variant associated with cardiofaciocutaneous syndrome activates the RAF-ERK pathway. *Front. Physiol.* **10**, 388 (2019).
25. O. Assossou et al., Characterization of an excreted/secreted antigen form of 14-3-3 protein in Toxoplasma gondii tachyzoites. *FEMS Microbiol. Lett.* **234**, 19–25 (2004).
26. C. Vincenz, V. M. Dixit, 14-3-3 proteins associate with A20 in an isoform-specific manner and function both as chaperone and adapter molecules. *J. Biol. Chem.* **271**, 20029–20034 (1996).
27. C. Aguilera et al., Efficient nuclear export of p65-IkappaBalpha complexes requires 14-3-3 proteins. *J. Cell Sci.* **119**, 3695–3704 (2006).
28. R. Kobayashi et al., 14-3-3 zeta protein secreted by tumor associated monocytes/macrophages from ascites of epithelial ovarian cancer patients. *Cancer Immunol. Immunother.* **58**, 247–258 (2009).
29. S. Dovrat et al., 14-3-3 and β-catenin are secreted on extracellular vesicles to activate the oncogenic Wnt pathway. *Mol. Oncol.* **8**, 894–911 (2014).

www.manaraa.com

30. B. Zhang et al., HucMSC exosome-delivered 14-3-3ζ orchestrates self-control of the wnt response via modulation of YAP during cutaneous regeneration. *Stem Cells* **34**, 2485–2500 (2016).

31. R. Chakravarti et al., 14-3-3 in thoracic aortic aneurysms: Identification of a novel autoantigen in large vessel vasculitis. *Arthritis Rheumatol.* **67**, 1913–1921 (2015).

32. J. McGowan, C. Peter, S. Chattopadhyay, R. Chakravarti. 14-3-3zeta: A novel immunogen promotes inflammatory cytokine production. *Front. Immunol.* **10**, 1553 (2019).

33. J. Holmberg et al., Pristane, a non-antigenic adjuvant, induces MHC class II-restricted, arthritogenic T cells in the rat. *J. Immunol.* **176**, 1172–1179 (2006).

34. J. Tuncel et al., Animal models of rheumatoid arthritis (I): Pristane-induced arthritis in the rat. *PLoS One* **11**, e0155936 (2016).

35. M. Brenner et al., The non-MHC quantitative trait locus Cia5 contains three major arthritis genes that differentially regulate disease severity, pannus formation, and joint damage in collagen- and pristane-induced arthritis. *J. Immunol.* **174**, 7894–7903 (2005).

36. J. McGowan et al., 14-3-3ζ-TRAF5 axis governs interleukin-17A signaling. *Proc. Natl. Acad. Sci. U.S.A.* **117**, 25008–25017 (2020).

37. P. S. Cheah et al., Neurodevelopmental and neuropsychiatric behaviour defects arise from 14-3-3ζ deficiency. *Mol. Psychiatry* **17**, 451–466 (2012).

38. X. Xu et al., 14-3-3ζ deficient mice in the BALB/c background display behavioural and anatomical defects associated with neurodevelopmental disorders. *Sci. Rep.* **5**, 12434 (2015).

39. J. E. McGowan et al., Bioinformatic analysis reveals new determinants of antigenic 14-3-3 proteins and a novel antifungal strategy. *PLoS One* **12**, e0189503 (2017).

40. D. L. Asquith, A. M. Miller, I. B. McInnes, F. Y. Liew, Animal models of rheumatoid arthritis. *Eur. J. Immunol.* **39**, 2040–2044 (2009).

41. B. Joe, Quest for arthritis-causative genetic factors in the rat. *Physiol. Genomics* **27**, 1–11 (2006).

42. B. W. Kirkham et al., Synovial membrane cytokine expression is predictive of joint damage progression in rheumatoid arthritis: A two-year prospective study (the DAMAGE study cohort). *Arthritis Rheum.* **54**, 1122–1131 (2006).

43. D. M. Roeleveld, M. I. Koenders, The role of the Th17 cytokines IL-17 and IL-22 in rheumatoid arthritis pathogenesis and developments in cytokine immunotherapy. *Cytokine* **74**, 101–107 (2015).

44. C. A. Dinarello, Interleukin-1 in the pathogenesis and treatment of inflammatory diseases. *Blood* **117**, 3720–3732 (2011).

45. C. C. Munier, C. Ottmann, M. W. D. Perry, 14-3-3 modulation of the inflammatory response. *Pharmacol. Res.* **105236**, (2021).

46. A. Matta, K. W. Siu, R. Ralhan, 14-3-3 zeta as novel molecular target for cancer therapy. *Expert Opin. Ther. Targets* **16**, 515–523 (2012).

47. F. Moghaddas et al., A novel pyrin-associated autoinflammation with neutrophilic dermatosis mutation further defines 14-3-3 binding of pyrin and distinction to familial Mediterranean fever. *Ann. Rheum. Dis.* **76**, 2085–2094 (2017).

48. E. Y. Kim, K. D. Moudgil, The determinants of susceptibility/resistance to adjuvant arthritis in rats. *Arthritis Res. Ther.* **11**, 239 (2009).

49. S. Herman et al., Cell death and cytokine production induced by autoimmunogenic hydrocarbon oils. *Autoimmunity* **45**, 602–611 (2012).

50. E. Schurgers, A. Billiau, P. Matthys, Collagen-induced arthritis as an animal model for rheumatoid arthritis: Focus on interferon-γ. *J. Interferon Cytokine Res.* **31**, 917–926 (2011).

51. J. Tuncel, S. Haag, R. Holmdahl, MHC class II alleles associated with Th1 rather than Th17 type immunity drive the onset of early arthritis in a rat model of rheumatoid arthritis. *Eur. J. Immunol.* **47**, 563–574 (2017).

52. C. Patten et al., Characterization of pristane-induced arthritis, a murine model of chronic disease: Response to antirheumatic agents, expression of joint cytokines, and immunopathology. *Arthritis Rheum.* **50**, 3334–3345 (2004).

53. C. Wang et al., IL-17 induced NOTCH1 activation in oligodendrocyte progenitor cells enhances proliferation and inflammatory gene expression. *Nat. Commun.* **8**, 15508 (2017).

54. H. Cai, H. J. Sun, Y. H. Wang, Z. Zhang, Relationships of common polymorphisms in IL-6, IL-1A, and IL-1B genes with susceptibility to osteoarthritis: A meta-analysis. *Clin. Rheumatol.* **34**, 1443–1453 (2015).

55. K. Shimizu et al., IL-1 receptor type 2 suppresses collagen-induced arthritis by inhibiting IL-1 signal on macrophages. *J. Immunol.* **194**, 3156–3168 (2015).

56. D. E. Furst, Anakinra: Review of recombinant human interleukin-I receptor antagonist in the treatment of rheumatoid arthritis. *Clin. Ther.* **26**, 1960–1975 (2004).

57. M. Noack, P. Miossec, Selected cytokine pathways in rheumatoid arthritis. *Semin. Immunopathol.* **39**, 365–383 (2017).

58. I. Auger et al., New autoantigens in rheumatoid arthritis (RA): Screening 8268 protein arrays with sera from patients with RA. *Ann. Rheum. Dis.* **68**, 591–594 (2009).

59. B. J. Prakken et al., Epitope-specific immunotherapy induces immune deviation of proinflammatory T cells in rheumatoid arthritis. *Proc. Natl. Acad. Sci. U.S.A.* **101**, 4228–4233 (2004).

60. M. H. Hoffmann et al., The rheumatoid arthritis-associated autoantigen hnRNP-A2 (RA33) is a major stimulator of autoimmunity in rats with pristane-induced arthritis. *J. Immunol.* **179**, 7568–7576 (2007).

61. B. Joe, M. M. Griffiths, E. F. Remmers, R. L. Wilder, Animal models of rheumatoid arthritis and related inflammation. *Curr. Rheumatol. Rep.* **1**, 139–148 (1999).

62. K. Kannan, R. A. Ortmann, D. Kimpel, Animal models of rheumatoid arthritis and their relevance to human disease. *Pathophysiology* **12**, 167–181 (2005).

63. P. Wernhoff, P. Olofsson, R. Holmdahl, The genetic control of rheumatoid factor production in a rat model of rheumatoid arthritis. *Arthritis Rheum.* **48**, 3584–3596 (2003).

64. F. Ingegnoli, R. Castelli, R. Gualtierotti, Rheumatoid factors: Clinical applications. *Dis. Markers* **35**, 727–734 (2013).

65. J. Zhang et al., Protective efficacy and mechanism of passive immunization with polyclonal antibodies in a sepsis model of *Staphylococcus aureus* infection. *Sci. Rep.* **5**, 15553 (2015).

66. A. Kistner et al., Characteristics of autoantibodies targeting 14-3-3 proteins and their association with clinical features in newly diagnosed giant cell arteritis. *Rheumatology (Oxford)* **56**, 829–834 (2017).

67. A. Kaplan, M. Bueno, A. E. Fournier, Extracellular functions of 14-3-3 adaptor proteins. *Cell. Signal.* **31**, 26–30 (2017).

68. M. Chimen et al., Homeostatic regulation of T cell trafficking by a B cell-derived peptide is impaired in autoimmune and chronic inflammatory disease. *Nat. Med.* **21**, 467–475 (2015).

69. J. S. Kong et al., Dynamic transcriptome analysis unveils key proresolving factors of chronic inflammatory arthritis. *J. Clin. Invest.* **130**, 3974–3986 (2020).

70. J. J. Yu et al., An essential role for IL-17 in preventing pathogen-initiated bone destruction: Recruitment of neutrophils to inflamed bone requires IL-17 receptor-dependent signals. *Blood* **109**, 3794–3802 (2007).

71. J. Goswami, N. Hernández-Santos, L. A. Zuniga, S. L. Gaffen, A bone-protective role for IL-17 receptor signaling in ovariectomy-induced bone loss. *Eur. J. Immunol.* **39**, 2831–2839 (2009).

72. T. Assis-Ribas, M. F. Forni, S. M. B. Winnischofer, M. C. Sogayar, M. Trombetta-Lima, Extracellular matrix dynamics during mesenchymal stem cells differentiation. *Dev. Biol.* **437**, 63–74 (2018).

73. A. Peinnequin et al., Rat pro-inflammatory cytokine and cytokine related mRNA quantification by real-time polymerase chain reaction using SYBR green. *BMC Immunol.* **5**, 3 (2004).

Kim et al.
14-3-3ζ: A suppressor of inflammatory arthritis

www.manaraa.com